医薬品
医薬部外品　研究報告 調査報告書
化粧品

識別番号・報告回数			報告日	第一報入手日	新医薬品等の区分	機構処理欄
				2004.12.1	該当なし	
一般的名称	人血清アルブミン		研究報告の公表状況	Science, 2004;306(5702). 1692-1693	公表国 英国	
販売名(企業名)	赤十字アルブミン２０（日本赤十字社） 赤十字アルブミン２５（日本赤十字社）					

研究報告の概要

変異型クロイツフェルトヤコブ病（vCJD）は、非常に特徴的な臨床病態と分子形態を有するヒトプリオン病であり、ウシ海綿状脳症（BSE）の感染と関連がある。今回、トランスジェニックマウスがこの表現型を呈示するためには、129 位のアミノ酸がメチオニンであるヒトプリオン蛋白質（prion protein : PrP）の発現が必要であることを発見した。129 位のアミノ酸がバリンであるヒト PrP をトランスジェニックマウスに発現させると、臨床病理学的に異なるフェノタイプが生じ、BSE 由来プリオンの伝播を阻止し、この伝播阻止は、次世代でも受け継がれた。ヒト PrP の 129 位の残基多型が、BSE プリオン感染後のプリオンの臨床病理学的なフェノタイプの発現に影響を与えた。従って、ヒトにおける一次的および二次的な BSE 由来プリオン感染がプリオン種やレシピエントの遺伝子型に依存して、散発的な CJD 様表現型や vCJD に依存して新規の表現型をもたらすかもしれない。

報告企業の意見	今後の対応
先に、大腸菌（*Escherichia coli*）で作製した組換えマウスプリオン蛋白質（recMoPrP）を用いた感染実験により、プリオン病が発症したことから、プリオン蛋白質自体に感染性があることを示唆する報告を行っている。今般、ヒトにおける一次的および二次的な BSE 由来プリオン感染は、プリオン種やレシピエントの遺伝子型に依存して、散発的な CJD 様表現型や vCJD に依存して新規の表現型をもたらす可能性があるとの報告である。	これまでの疫学研究等では、血漿分画製剤を介して vCJD が伝播するという証拠はない。また異常プリオンがアルブミン製剤の製造工程で効果的に除去されるとの報告もあるが、感染リスクを完全には排除できないため、今後も情報の収集に努める。

使用上の注意記載状況・その他参考事項等

赤十字アルブミン２０
赤十字アルブミン２５
血液を原料とすることに由来する感染症伝播等

6. H.-W. Park, S.-T. Kim, A. Sancar, J. Deisenhofer, *Science* 268, 1866 (1995).
7. K. S. Christine, A. W. MacFarlane IV, K. Yank, R. J. Stanley, *J. Biol. Chem.* 277, 38339 (2002).
8. B. J. Vande Berg, G. B. Sancar, *J. Biol. Chem.* 273, 20276 (1998).
9. D. B. Sanders, O. Wiest, *J. Am. Chem. Soc.* 121, 5127 (1999).
10. J. Antony, D. M. Medvedev, A. A. Stuchebrukhov, *J. Am. Chem. Soc.* 122, 1057 (2000).
11. T. Torizawa *et al.*, *J. Biol. Chem.* 279, 32950 (2004).
12. K. Miki *et al.*, *J. Mol. Biol.* 233, 167 (1993).
13. Materials and methods are available as supporting material on *Science* Online.
14. J. Butenandt *et al.*, *Chem. Eur. J.* 6, 62 (2000).
15. I. Husain, J. Griffith, A. Sancar, *Proc. Natl. Acad. Sci. U.S.A.* 85, 2558 (1988).
16. H. Park *et al.*, *Proc. Natl. Acad. Sci. U.S.A.* 99, 15965 (2002).
17. D. G. Vassylyev *et al.*, *Cell* 83, 773 (1995).
18. Single-letter abbreviations for the amino acid residues are as follows: A, Ala; C, Cys; D, Asp; E, Glu; F, Phe; G, Gly; H, His; I, Ile; K, Lys; L, Leu; M, Met; N, Asn; P, Pro; Q, Gln; R, Arg; S, Ser; T, Thr; V, Val; W, Trp; and Y, Tyr.
19. I. Husain, G. B. Sancar, S. R. Holbrook, A. Sancar, *J. Biol. Chem.* 262, 13188 (1987).
20. A. Kiener, I. Husain, A. Sancar, C. Walsh, *J. Biol. Chem.* 264, 13880 (1989).
21. T. Langenbacher *et al.*, *J. Am. Chem. Soc.* 119, 10532 (1997).
22. A. Pezeshk, I. D. Podmore, P. F. Heelis, M. C. R. Symons, *J. Phys. Chem.* 100, 19714 (1996).
23. H. Ling, F. Boudsocq, B. S. Plosky, R. Woodgate, W. Yang, *Nature* 424, 1083 (2003).
24. R. Kort, H. Komori, S. Adachi, K. Miki, A. P. M. Eker, *Acta Crystallogr.* D60, 1205 (2004).
25. J. Rak, A. A. Voityuk, M.-E. Michel-Beyerle, N. Rösch, *J. Phys. Chem. A* 103, 3569 (1999).
26. J. Hahn, M. E. Michel-Beyerle, N. Rösch, *J. Phys. Chem. B* 103, 2001 (1999).
27. S. Weber, K. Möbius, G. Richter, C. W. M. Kay, *J. Am. Chem. Soc.* 123, 3790 (2001).
28. D. Medvedev, A. A. Stuchebrokhov, *J. Theor. Biol.* 210, 237 (2001).

29. We thank A. Yasui for provision of the *A. nidulans* photolyase expression construct; J. Bosch for help with data collection; C. Schulze-Briese for support at synchrotron beamline X06SA, Swiss Light Source, Villingen, Switzerland, and P. Tucker at beamline BW7A, European Molecular Biology Laboratory, Hamburg, Germany; and J. H. J. Hoeijmakers for his continuing interest. Supported by the Deutsche Forschungsgemeinschaft, Volkswagen Foundation, Fonds der chemischen Industrie, and the Boehringer Ingelheim Fonds. Coordinates and structure factors of the photolyase/CPD-DNA complex are deposited in the Research Collaboratory for Structural Bioinformatics protein data bank (accession no. 1TEZ).

Supporting Online Material
www.sciencemag.org/cgi/content/full/306/5702/1789/DC1
Materials and Methods
Figs. S1 and S2
Table S1
References and Notes

17 June 2004; accepted 18 October 2004

Human Prion Protein with Valine 129 Prevents Expression of Variant CJD Phenotype

Jonathan D. F. Wadsworth, Emmanuel A. Asante, Melanie Desbruslais, Jacqueline M. Linehan, Susan Joiner, Ian Gowland, Julie Welch, Lisa Stone, Sarah E. Lloyd, Andrew F. Hill,* Sebastian Brandner, John Collinge†

Variant Creutzfeldt-Jakob disease (vCJD) is a unique and highly distinctive clinicopathological and molecular phenotype of human prion disease associated with infection with bovine spongiform encephalopathy (BSE)–like prions. Here, we found that generation of this phenotype in transgenic mice required expression of human prion protein (PrP) with methionine 129. Expression of human PrP with valine 129 resulted in a distinct phenotype and, remarkably, persistence of a barrier to transmission of BSE-derived prions on subpassage. Polymorphic residue 129 of human PrP dictated propagation of distinct prion strains after BSE prion infection. Thus, primary and secondary human infection with BSE-derived prions may result in sporadic CJD-like or novel phenotypes in addition to vCJD, depending on the genotype of the prion source and the recipient.

Distinct prion strains are associated with biochemically distinct forms of disease-related prion protein (PrP^{Sc}). Four PrP^{Sc} types have been observed in brain tissue from patients with distinct Creutzfeldt-Jakob disease (CJD) phenotypes: types 1 to 3 in classical (sporadic or iatrogenic) CJD and type 4 in vCJD (*1–3*). Polymorphism at residue 129 of human PrP (where either methionine or valine can be encoded) powerfully affects genetic susceptibility to human prion diseases (*4–7*) and appears to critically influence the propagation of these human PrP^{Sc} types. So far, types 1 and 4 PrP^{Sc} have been found only in humans homozygous for Met^{129}; type 3 PrP^{Sc} is seen almost exclusively in individuals with at least one valine allele; and type 2 PrP^{Sc} has been commonly observed in all codon 129 genotypes (*1–3*). BSE and vCJD prion infection in transgenic mice expressing human PrP, but not mouse PrP (*1*, *8–10*), indicates that codon 129 polymorphism determines the ability of human PrP to form type 4 PrP^{Sc} and to generate the neuropathological phenotype of vCJD.

Challenge of transgenic mice expressing human PrP Met^{129} (129MM Tg35 and 129MM Tg45 mice) with BSE and vCJD prions (*11*) resulted in faithful propagation of type 4 PrP^{Sc} (*10*) (Figs. 1 and 2) accompanied by the key neuropathological hallmark of vCJD, the presence of abundant florid PrP plaques (*10*). However, transgenic mice expressing human PrP Val^{129} (129VV Tg152 mice) responded quite differently. Although these 129VV Tg152 mice lack a transmission barrier to classical forms of CJD, regardless of the codon 129 genotype of the inoculum (*1*, *8*, *9*), the primary challenge with vCJD prions was characterized by a substantial transmission barrier to infection (only ~50% of inoculated mice were infected, compared with 100% of 129MM Tg35 and 129MM Tg45 mice) (Fig. 1; table S1). In addition, rather than type 4 PrP^{Sc}, vCJD-inoculated 129VV Tg152 mice propagated type 5 PrP^{Sc} (*9*), which shares the same predominance of the diglycosylated glycoform seen in type 4 PrP^{Sc} but is distinguished by proteinase K digestion products of greater molecular mass (Fig. 2A), which closely resemble those seen in human type 2 PrP^{Sc} (*9*). Type 5 PrP^{Sc} is associated with very weak diffuse PrP deposition in the brain (*9*), which contrasts markedly with the florid PrP plaques associated with the propagation of type 4 PrP^{Sc} in humans (*12*) or transgenic mice (*10*). Similar diffuse deposition of PrP is also observed in clinically affected BSE-inoculated 129VV Tg152 mice; however, type 5 PrP^{Sc} is undetectable in brain homogenate (*9*).

To further evaluate the molecular and neuropathological phenotype of vCJD- or BSE-inoculated 129VV Tg152 mice, we performed a second passage in the same breed of mice. Primary transmission of prions from one species to another is associated with a species or transmission barrier that is largely or completely abrogated on second and subsequent passage in the second species as the prions adapt to the new host. Second passage then resembles within-species transmission with a high (typically 100%) attack rate and much shortened and more consistent incubation period. It was remarkable, however, that such adaptation did not occur on second passage of BSE or vCJD prions in

Medical Research Council (MRC) Prion Unit and Department of Neurodegenerative Disease, Institute of Neurology, University College London, Queen Square, London WC1N 3BG, UK.

*Present address: Department of Biochemistry and Molecular Biology and Department of Pathology, University of Melbourne, Parkville, Victoria 3010, Australia.

†To whom correspondence should be addressed. E-mail: j.collinge@prion.ucl.ac.uk

129VV Tg152 mice. Brain inocula derived from four clinically affected BSE-inoculated 129VV Tg152 mice failed to transmit clinical disease or asymptomatic prion infection to additional 129VV Tg152 mice (Figs. 1 and 3; table S2). However, two of these inocula produced clinical prion disease (Fig. 3; table S2) with abundant PrP^{Sc} accumulation (fig. S1) on inoculation of wild-type FVB mice with incubation periods that are not compatible with persistence of the original BSE inoculum [supporting online material (SOM) text]. The prion strain generated in BSE-inoculated 129VV Tg152 mice was thus infectious in wild-type FVB mice, but not in additional 129VV Tg152 mice.

Valine 129 is unique to human PrP, and the failure of BSE prions to adapt in 129VV Tg152 mice on second passage contrasts sharply with the marked adaptation of BSE prions in FVB mice (Fig. 3; table S2) or in other murine (*13*) or primate (*14*) hosts that encode methionine at the corresponding position of PrP. BSE prions also efficiently adapt on second passage in 129MM Tg35 transgenic mice. Primary transmission of BSE prions in 129MM Tg35 mice resulted in bifurcation of propagated strain type and produced either type 2 or 4 PrP^{Sc} (Figs. 1 and 2) and neuropathology consistent with human sporadic CJD or vCJD, respectively (*10*). These distinct molecular and neuropathological phenotypes consistently "breed true" with very high efficiency on second passage in additional 129MM Tg35 transgenic mice (*15*). These findings contrast sharply with the complete lack of prion transmission on second passage of the same BSE inocula in 129VV Tg152 mice, supporting the interpretation that human PrP Val^{129} severely restricts propagation of the BSE prion strain.

This conclusion was further reinforced by study of the parameters of second passage of vCJD prions. As seen with second passage of BSE prions, clinical disease was observed only in FVB, and not in 129VV Tg152, recipients. Brain inocula from clinically affected, type 5 PrP^{Sc} positive, primary vCJD-inoculated 129VV Tg152 mice produced clinical prion disease (Fig. 3; table S2) and PrP^{Sc} accumulation (fig. S1) on subpassage in FVB mice, but produced only subclinical infection (with PrP^{Sc} accumulation) in 7 out of 11 inoculated 129VV Tg152 mice (Figs. 1 and 3). Notably, in four of these, high-sensitivity methods (*16*) were required to detect PrP^{Sc} in brain homogenate (table S2). Type 5 PrP^{Sc} was faithfully propagated on second passage in 129VV Tg152 mice (Fig. 2A). In the three mice containing the highest levels of type 5 PrP^{Sc}, extensive spongiosis was also observed (Fig. 4), and in one of these, in contrast to the pathology seen on first passage, numerous PrP plaques were seen (Fig. 4). Type 4 PrP^{Sc} is invariably associated with prominent florid plaques in the cortex of human vCJD brain (*12*) and in vCJD- or BSE-prion inoculated 129MM Tg35 and Tg45 transgenic mice (*10*), whereas plaques associated with type 5 PrP^{Sc} were restricted to the corpus callosum and had a nonflorid morphology (Fig. 4). The lack of adaptation of vCJD prions on second passage in 129VV Tg152 mice contrasted sharply with the behavior of

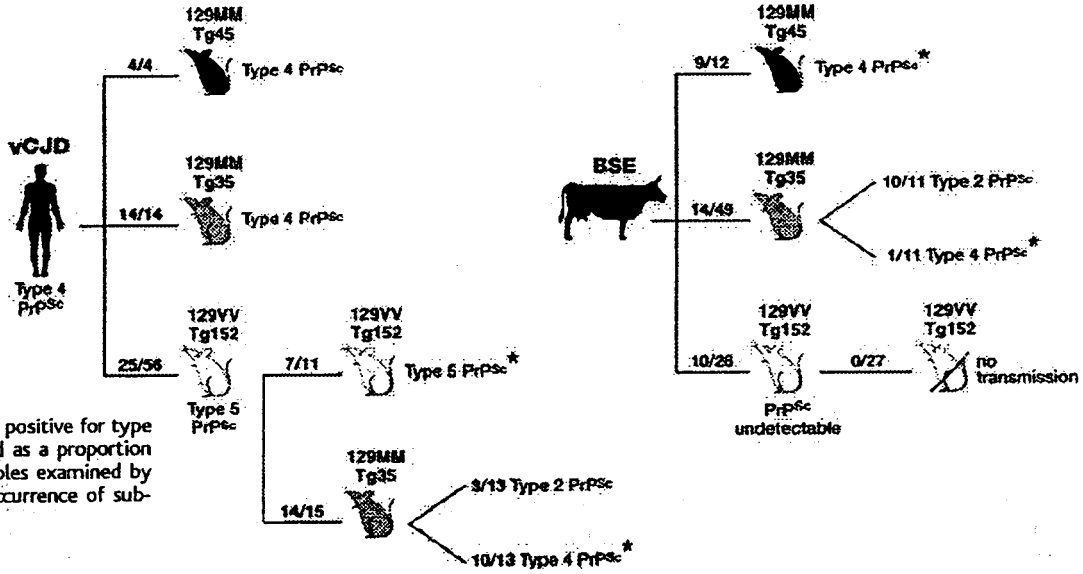

Fig. 1. Summary of transmissions of vCJD and BSE prions to transgenic mice. The total number of prion-affected mice (both clinical and subclinical) is reported for each inoculated group: 129MM Tg45 mice (black), 129MM Tg35 mice (gray), 129VV Tg152 mice (white). Animals were scored by clinical signs, immunoblotting, and/or immunohistochemistry. Primary transmission data have been published previously (*9*, *10*). In transmissions that result in bifurcation of propagated PrP^{Sc} type, the number of samples positive for type 2 or type 4 PrP^{Sc} is reported as a proportion of the total number of samples examined by immunoblotting. (*). The occurrence of subclinical prion infection only.

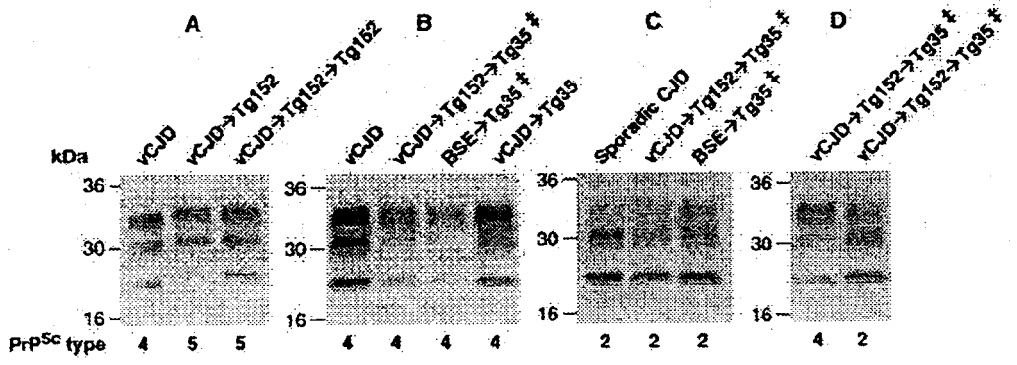

Fig. 2. Molecular strain typing of vCJD and BSE prion transmissions in transgenic mice. (A to D) Immunoblots of proteinase K–treated brain homogenates from variant and sporadic CJD (*PRNP* 129 MM genotype) and transgenic mice were analyzed by enhanced chemiluminescence with either monoclonal antibody 3F4 against PrP (A) or biotinylated monoclonal antibody ICSM 35 against PrP (B to D). The identity of the brain sample is designated above each lane with the type of PrP^{Sc} present in the sample designated below.
‡Transmissions that result in the propagation of either type 2 or type 4 PrP^{Sc}.

vCJD prions in wild-type FVB mice, where typical adaptation was observed on second passage with 100% clinical prion disease with abundant PrP^{Sc} accumulation (fig. S1) at markedly reduced incubation periods (Fig. 3; table S2).

Both BSE and vCJD prions failed to propagate efficiently on either primary or, remarkably, second passage, in 129VV Tg152 mice in sharp contrast to 129MM Tg mice or wild-type animals, and where detectable, infection was associated with a distinct PrP^{Sc} type and pathological phenotype. Thus, human PrP Val^{129} appears not to be a compatible substrate for propagation of the prion strain seen in vCJD. This interpretation was supported by the transmission properties of 129VV Tg152–passaged vCJD prions in 129MM Tg35 mice. Here, 14 out of 15 129MM Tg35 mice inoculated with isolates containing type 5 PrP^{Sc} showed PrP^{Sc} accumulation (Fig. 1; table S3), typically to much higher levels than seen in 129VV Tg152 mice receiving the same inocula. However, the PrP^{Sc} seen was not of the type 5 pattern but instead these transmissions mirrored the behavior of BSE prions in 129MM Tg35 mice (*10*), where, instead, either type 4 or type 2 PrP^{Sc} were seen (Figs. 1 and 2, B to D). Thus human PrP^{Sc} types 4 and 5 are restricted to propagating in mice expressing human PrP Met^{129} or Val^{129}, respectively.

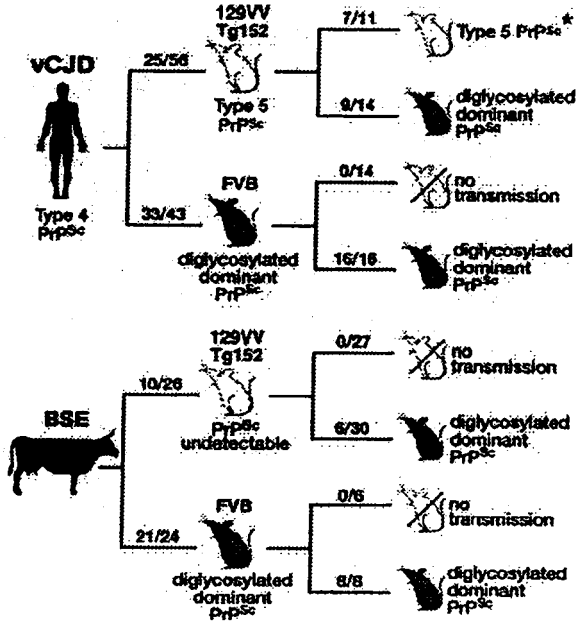

Fig. 3. Summary of transmissions of vCJD and BSE prions to transgenic and wild-type FVB mice. The total number of prion-affected mice (both clinical and subclinical) is reported for each inoculated group: 129VV Tg152 mice (white), wild-type FVB mice (gray). Animals were scored by clinical signs, immunoblotting, and/or immunohistochemistry. Data are derived from tables S1 and S2. (*), The occurrence of subclinical prion infection only.

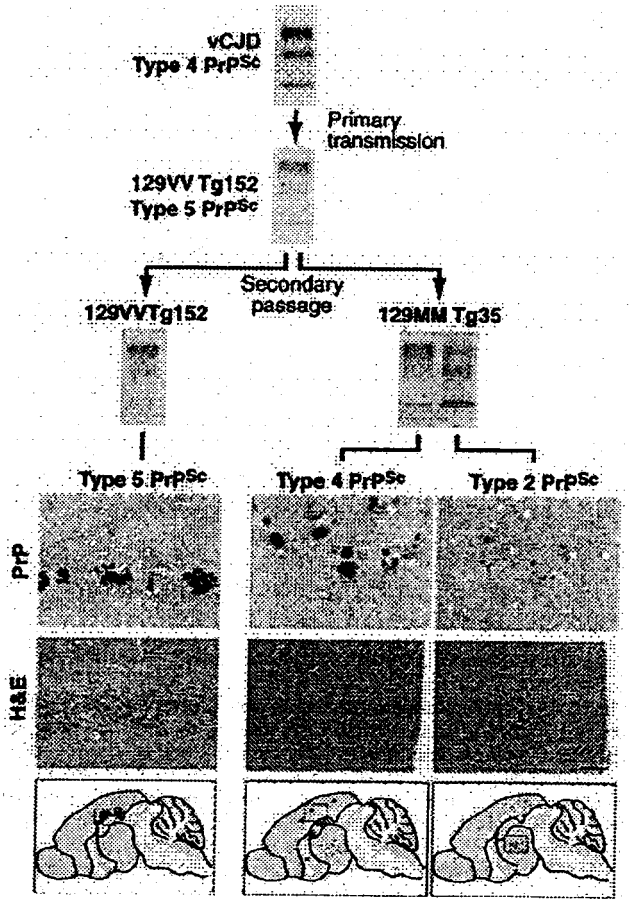

Fig. 4. Neuropathological analysis of transgenic mouse brain. Primary transmission of vCJD prions in 129VV Tg152 mice produces type 5 PrP^{Sc} that is maintained after secondary passage in 129VV Tg152 mice but induces propagation of either type 2 or type 4 PrP^{Sc} after passage in 129MM Tg35 mice. Immunohistochemistry (PrP) shows abnormal PrP immunoreactivity, including PrP-positive plaques, stained with monoclonal antibody 3F4 against PrP. Sections stained with hematoxylin-and-eosin (H&E) show spongiform neurodegeneration (left, corpus callosum; middle and right, parietal cortex). Scale bar, 100 μm. Lower panels show the regional distribution of abnormal PrP deposition. Green boxes in the sketches denote the area from which PrP-stained sections are derived.

In conclusion, we have demonstrated that BSE and vCJD prion infection in transgenic mice can result in the propagation of distinct molecular and neuropathological phenotypes dependent on host PrP residue 129 and possibly other, as yet unidentified, disease modifying loci (*10*). These data predict a critical role for *PRNP* codon 129 in governing the thermodynamic permissibility of human PrP^{Sc} conformation that can be interpreted within a conformational selection model of prion transmission barriers (*17–19*) (SOM text) and suggest that there is no overlapping preferred conformation for Val^{129} and Met^{129} human PrP that can be generated as a result of exposure to the vCJD/BSE prion strain. Biophysical measurements suggest that this powerful effect of residue 129 on prion strain selection is likely to be mediated by means of its effect on the conformation of PrP^{Sc} or its precursors or on the kinetics of their formation, as it has no measurable effect on the folding, dynamics, or stability of the normal cellular prion protein PrP^{C} (*20*).

Although caution must be exercised in extrapolating from animal models, even

where, as here, faithful recapitulation of molecular and pathological phenotypes is possible, our findings argue that primary human BSE prion infection, as well as secondary infection with vCJD prions by iatrogenic routes, may not be restricted to a single disease phenotype. These data, together with the recent recognition of probable iatrogenic transmission of vCJD prions to recipients of blood (*21*, *22*), including a *PRNP* codon 129 Met/Val heterozygous individual (*22*), reiterate the need to stratify all human prion disease patients by PrP^{Sc} type. This surveillance will facilitate rapid recognition of novel PrP^{Sc} types and of any change in relative frequencies of particular PrP^{Sc} subtypes in relation to either BSE exposure patterns or iatrogenic sources of vCJD prions.

References and Notes

1. J. Collinge, K. C. L. Sidle, J. Meads, J. Ironside, A. F. Hill, *Nature* 383, 685 (1996).
2. J. D. F. Wadsworth *et al.*, *Nature Cell Biol.* 1, 55 (1999).
3. A. F. Hill *et al.*, *Brain* 126, 1333 (2003).
4. J. Collinge, M. S. Palmer, A. J. Dryden, *Lancet* 337, 1441 (1991).
5. M. S. Palmer, A. J. Dryden, J. T. Hughes, J. Collinge, *Nature* 352, 340 (1991).
6. H. S. Lee *et al.*, *J. Infect. Dis.* 183, 192 (2001).
7. S. Mead *et al.*, *Science* 300, 640 (2003).
8. J. Collinge *et al.*, *Nature* 378, 779 (1995).
9. A. F. Hill *et al.*, *Nature* 389, 448 (1997).
10. E. A. Asante *et al.*, *EMBO J.* 21, 6358 (2002).
11. Materials and methods are available as supporting material on *Science* Online.
12. R. G. Will *et al.*, *Lancet* 347, 921 (1996).
13. M. Bruce *et al.*, *Philos. Trans. R. Soc. London Ser. B.* 343, 405 (1994).
14. C. I. Lasmezas *et al.*, *Proc. Natl. Acad. Sci. U.S.A.* 98, 4142 (2001).
15. E. A. Asante, J. D. F. Wadsworth, J. Collinge, unpublished observations. These data will be reported in full elsewhere.
16. J. D. F. Wadsworth *et al.*, *Lancet* 358, 171 (2001).
17. J. Collinge, *Lancet* 354, 317 (1999).
18. J. Collinge, *Annu. Rev. Neurosci.* 24, 519 (2001).
19. A. F. Hill, J. Collinge, *Trends Microbiol.* 11, 578 (2003).
20. L. L. Hosszu *et al.*, *J. Biol. Chem.* 279, 28515 (2004).
21. C. A. Llewelyn *et al.*, *Lancet* 363, 417 (2004).
22. A. H. Peden, M. W. Head, D. L. Ritchie, J. E. Bell, J. W. Ironside, *Lancet* 364, 527 (2004).

23. We thank C. Brown and his team for animal care, R. Young for preparation of figures, and K. Fox and S. Cooper for technical assistance. We especially thank all patients and their families for generously consenting to use of human tissues in this research, and the UK neuropathologists who have kindly helped in providing these tissues. We thank R. Bradley, D. Matthews, S. A. C. Hawkins and colleagues at the UK Veterinary Laboratories Agency for providing BSE tissues. This work was funded by the UK Medical Research Council and European Commission. One of the routine antibodies used in this work (ICSM 35) is marketed by D-Gen Ltd., an academic spin-off company. J.C. is a director of D-Gen and J.C., J.D.F.W., and A.F.H. are shareholders and consultants of D-Gen.

Supporting Online Material

www.sciencemag.org/cgi/content/full/1103932/DC1
Materials and Methods
SOM Text
Fig. S1
Tables S1 to S3
References and Notes

11 August 2004; accepted 21 October 2004
Published online 11 November 2004;
10.1126/science.1103932
Include this information when citing this paper.

Rescue of Dystrophic Muscle Through U7 snRNA–Mediated Exon Skipping

Aurélie Goyenvalle,[1] Adeline Vulin,[1] Françoise Fougerousse,[1] France Leturcq,[2] Jean-Claude Kaplan,[2] Luis Garcia,[1] Olivier Danos[1]*

Most mutations in the dystrophin gene create a frameshift or a stop in the mRNA and are associated with severe Duchenne muscular dystrophy. Exon skipping that naturally occurs at low frequency sometimes eliminates the mutation and leads to the production of a rescued protein. We have achieved persistent exon skipping that removes the mutated exon on the dystrophin messenger mRNA of the *mdx* mouse, by a single administration of an AAV vector expressing antisense sequences linked to a modified U7 small nuclear RNA. We report the sustained production of functional dystrophin at physiological levels in entire groups of muscles and the correction of the muscular dystrophy.

Duchenne muscular dystrophy (DMD) is an X-linked recessive disorder caused by mutations in a gene that encodes dystrophin, a large cytoskeletal protein that complexes with other partners at the sarcolemma and is essential for membrane integrity of the muscle fiber. The dystrophin gene spans about 2.5 Mb and encodes a major 14-kb mRNA transcript processed from 79 exons. Full-length dystrophin (427 kD) is composed of several domains consisting of an actin-binding site at the N terminus; a central rod domain of 24 spectrin-like repeats; and a cysteine-rich domain, which binds other

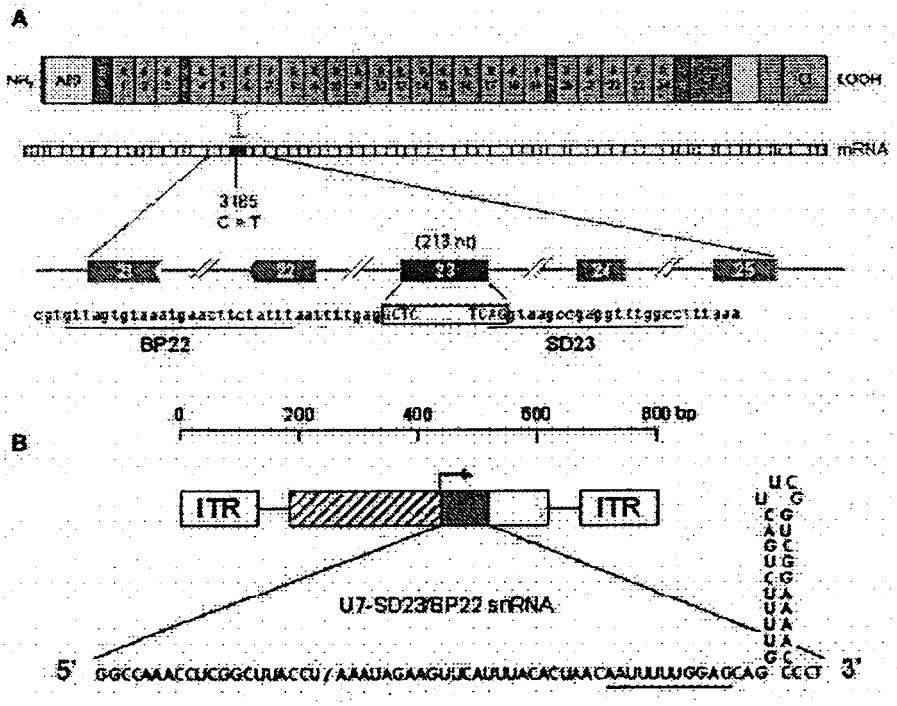

Fig. 1. (A) (Top) Dystrophin includes an actin-binding domain (ABD) at the N terminus, a central rod domain that contains 24 spectrin-like repeats (R) and four hinge segments (H), a β-dystroglycan binding, a cysteine-rich domain (CR), and a C-terminal domain (CT). (Middle) Position of exon 23 partly encoding repeats R5 and R6 in which a C to T mutation creates a stop codon in the *mdx* mouse. (Bottom) Target sequences for exon skipping at the branch point (BP22) upstream of exon 23 and at the downstream donor splice site (SD23). (**B**) Structure of the AAV(U7-SD23/BP22) vector. The U7-SD23/BP22 cassette includes the U7-promoter (position −267 to +1, hatched box), the U7SmOPT snRNA (gray box and sequence below) and downstream sequences down to position 116 (open box). It is shown between two AAV2 inverted terminal repeats (ITRs).